Organic Electronics 38 (2016) 350–356

Contents lists available at ScienceDirect

Organic Electronics

journal homepage: www.elsevier.com/locate/orgel

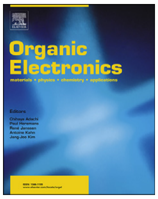

In situ implanting carbon nanotube-gold nanoparticles into ZnO as efficient nanohybrid cathode buffer layer for polymer solar cells

Ting Hu [a, 1], Longbin Li [a], Shuqin Xiao [a, b, 1], Kai Yuan [a, b], Hanjun Yang [a], Lie Chen [a, b, **], Yiwang Chen [a, b, *]

[a] College of Chemistry/Institute of Polymers, Nanchang University, 999 Xuefu Avenue, Nanchang 330031, China
[b] Jiangxi Provincial Key Laboratory of New Energy Chemistry, Nanchang University, 999 Xuefu Avenue, Nanchang 330031, China

ARTICLE INFO

Article history:
Received 30 June 2016
Received in revised form
24 August 2016
Accepted 12 September 2016
Available online 17 September 2016

Keywords:
In situ
Nanohybrids
Carbon nanotube
Plasmonic
Polymer solar cell

ABSTRACT

ZnO, plasmonic gold nanoparticles and conductive carbon nanotubes were combined by in situ growing to improve the light absorption and the electron mobility and the performance of polymer solar cells. Gold nanoparticles decorated carboxylic CNT (CNT-Au) was prepared by simple dehydration-condensation reaction. While CNT provides the template for the in situ growth of ZnO to form homogeneous film with less defects and higher conductivity, gold nanoparticles induce the surface plasmon effect to increase the light absorption. Compared to the bare ZnO, ZnO@CNT-Au nanohybrids could increase photo-generated excitons, decrease the charge recombination and facilitate the electron collection. In consequence, the power conversion efficiency of inverted polymer solar cell based on thieno [3,4-b]thiophene/benzodithiophene (PTB7) [6,6]:— phenyl C_{71}-butyric acid methyl ester ($PC_{71}BM$) was improved to 7.9% by adopting ZnO@CNT-Au as cathode buffer layer.

1. Introduction

Polymer solar cells (PSCs) have attracted enormous attention as the most promising source of green energy for the future because of their light weight, low-cost solution processability and printable for large-scale fabrication by roll-to-roll techniques [1–4]. Generally, the PSCs are fabricated based on a bulk heterojunction of conjugated polymers and fullerenes as the photoactive layer. Good absorptivity and stability of the device structure and material are essential to achieve an idea solar cell. In order to get rid of the hygroscopic and acid poly(3,4-ethylenedioxythiophene):poly-(styrene sulfonic acid) (PEDOT:PSS) and the air sensitive Al cathode, inverted architecture are employed widely [5–7]. ZnO has been used as cathode buffer layer in inverted PSCs with suitable energy levels, good optical transmittance, high electron mobility, excellent stability [8–10]. It is known that ZnO nanoparticles synthesized by using sol–gel precursors or colloidal nanocrystals are full of surface defects, which can decrease the photocurrent and the charge selectivity of cathode contacts [11–13]. Since high conductivity can reduce the voltage drop across the interfacial layers and facilitate the charge dissociation [14], the conductivity of the interfacial material should be improved.

Carbon nanomaterials such as fullerenes, carbon nanotubes (CNTs), and graphene have often been employed into metal oxides buffer layer to improve the charge mobility [15–19], due to their excellent electron affinity [20–24]. Among them, CNTs have been attracted the most attention for their excellent physical and chemical properties. CNTs have a large aspect ratio and high charge mobility with one-dimensional structure. In addition, localized surface plasmonic resonance (LSPR) of the metal nanoparticles is an effective way to enhance the light absorption and generates excess excitons in the organic active layer by increasing electromagnetic field [25–27]. In theory, blending metal nanoparticles into the organic active layer is the best way to obtain the highest light harvesting. Unfortunately, the metal particles become recombination centers, trapping free charge carriers and retarding charge transport [28]. To solve this problem, metal nanoparticles are incorporated into the interface layer, such as PEDOT:PSS [29], ZnO [30] TiO_x [31] and graphene [32].

Herein, a novel ZnO@CNT-Au nanohybrids by in situ growth of ZnO nanoparticles in gold nanoparticles decorated carboxylic CNT

---

* Corresponding author. College of Chemistry/Institute of Polymers, Nanchang University, 999 Xuefu Avenue, Nanchang 330031, China.
** Corresponding author. College of Chemistry/Institute of Polymers, Nanchang University, 999 Xuefu Avenue, Nanchang 330031, China.
E-mail addresses: chenlie@ncu.edu.cn (L. Chen), ywchen@ncu.edu.cn (Y. Chen).

[1] T. Hu and S. Xiao contributed equally to this work.

http://dx.doi.org/10.1016/j.orgel.2016.09.015

(CNT-Au) has been developed as cathode buffer layer for improving polymer solar cells performance. For the ZnO@CNT-Au nanohybrids, the carboxylic CNT provides a template for the in situ growth of ZnO nanoparticles, forming a homogeneous film with less defects and higher conductivity. Besides, gold nanoparticles were adopted to decorate carboxylic CNT, inducing the surface plasmon effect. Compared to bare ZnO, ZnO@CNT-Au possesses the higher electron mobility with a decreased work function, which could promote the charge dissociation. Meanwhile, ZnO@CNT-Au could increase photo-generated excitons with stronger light harvesting. As a result, the inverted polymer solar cells prepared from thieno [3,4-b]-thiophene/benzodithiophene (PTB7) donor and [6,6]-phenyl C_{71}-butyric acid methyl ester ($PC_{71}BM$) acceptor achieved a higher power conversion efficiency of 7.9% with ZnO@CNT-Au as cathode buffer layer.

2. Experimental

2.1. Synthesis of gold nanoparticles decorated carboxylic CNT (CNT-Au)

Gold nanoparticles decorated carboxylic CNT (CNT-Au) was prepared by simple dehydration-condensation reaction between CNT-COOH and Au-NH_2. CNT-COOH powders were dispersion in deionized (DI) water (0.3 mg/ml) by ultrasonication more than 4 h. Au-NH_2 was added into the CNT-COOH dispersion and was stirred at 50 °C for 30 min for dehydration-condensation reaction. Then, the resultant dispersion was vacuum filtered and dried.

2.2. Preparation of the ZnO@CNT-Au precursor

The ZnO was synthesized following the process reported by Heeger et al. [33] The general procedure for the preparation of ZnO as follows: the ZnO precursor was prepared by dissolving zinc acetate dihydrate ($Zn(CH_3COO)_2\cdot 2H_2O$, Aldrich, 99.9%, 1 g) and ethanolamine ($NH_2CH_2CH_2OH$, Aldrich, 99.5%, 0.28 g) in 2-methoxyethanol ($CH_3OCH_2CH_2OH$, Aldrich, 99.8%, 10 mL) under vigorous stirring for 12 h for the hydrolysis reaction in air. 0.6% wt CNT-Au was added to the ZnO precursor solution to obtain ZnO@CNT-Au precursor. Meanwhile, CNT-COOH with the same amount were added to the ZnO precursor solution to obtain ZnO@CNT-COOH precursor respectively for comparison.

2.3. Fabrication of inverted polymer solar cells

ITO-coated glass substrates (35 Ω·cm-2) were cleaned with alcohol, detergent, deionized water and isopropyl, and dried by nitrogen flow followed by plasma treatment for 15 min. After cleansing, ZnO, ZnO@CNT-COOH and ZnO@CNT-Au precursor solutions were then spin coated on top of the ITO/glass substrates as cathode buffer layers, and annealed in air for 1 h. The blended solution P3HT:$PC_{61}BM$ (11: w/w, 1,2-dichlorobenzene, 60 °C) or PTB7:$PC_{71}BM$ (11.5: w/w, chlorobenzene/1,8-diiodooctane (97:3 v/v), 70 °C) were stirred in glovebox overnight, which was spin coated on top of the cathode buffer layer as active layer. Finally, anode buffer layer MoO_3 (8 nm) and anode Ag (90 nm) was deposited on the top of the active layer by thermal evaporation in a high vacuum ($<10^{-7}$ Torr). The active device area was 4 mm^2. Current-voltage (*J-V*) characteristics were tested using Keithley 2400 Source Meter in the dark and under simulated AM 1.5 G (100 mW cm^{-2}) irradiation (Abet Solar Simulator Sun2000). Incident photon-to-current efficiency (IPCE) were measured under monochromatic illumination (Oriel Cornerstone 260 1/4 m monochromator equipped with Oriel 70613NS QTH lamp), and the calibration of the incident light was performed with a monocrystalline silicon diode.

2.4. Characterization

Ultraviolet–visible (UV–vis) absorption spectra and diffuse reflectance spectra were carried out by PerkinElmer Lambda 750 spectrophotometer. Hitachi F-7000 spectrofluorophotometer was applied for the measurements of photoluminescence (PL). The crystallinity of the samples were studied by the X-ray diffraction (XRD), using a Bruker D8 Focus X-ray diffractometer operating at 30 kV and 20 mA with a copper target ($\lambda = 1.54$ Å) under a scanning rate of 1°/min. The morphologies of all samples were measured by an atomic force microscope (AFM) (Digital Instrument Nanoscope 31), and a scanning electron microscopy (SEM, FEI Quanta 200F) and a transmission electron microscopy (TEM; JEOL, JEM-2100F, field emission transmission electron microscope) which were recorded on holey carbon-coated copper grids. Ultraviolet photoelectron spectroscopy (UPS) and X-ray photoelectron spectroscopy (XPS) measurements were carried out by AXIS-ULTRA DLD spectrometer (Kratos Analytical Ltd.) using He (I) (21.2 eV) as monochromatic light source. The thicknesses of all the layers were measured by surface profilometry (Alpha-Step-IQ). Water contact angle measurements for all samples were taken on JC2000A contact angle instrument.

3. Results and discussion

The inverted architecture of the device and the schematic diagram of ZnO@CNT-Au nanohybrids are shown in Fig. 1a. The chemical structures of the active materials used for device fabrication are displayed in Fig. 1b. Gold nanoparticles decorated carboxylic CNT (CNT-Au) was prepared by simple dehydration-condensation reaction between carboxylic CNT (CNT-COOH) and Au nanoparticles with amine groups (Au-NH_2). Compared to CNT-COOH, the Au nanoparticles are bound with CNTs homogeneously for CNT-Au, demonstrated by scanning electron microscopy (SEM) measurement (Fig. 2). As presented in Fig. S1, the lattice fringes for the (111) planes of Au nanoparticle (0.23 nm) and graphite stacking of CNT (0.34 nm) are evident.

ZnO@CNT nanohybrids were prepared from precursor with CNT by hydrolysis and the detailed process was provided in the supporting information. Due to the special one-dimensional structure, CNT could form a network sheet to provide the template for the in situ growth of ZnO nanoparticles. In order to investigate the effect of CNT on the growth of ZnO, atomic force microscopy (AFM) analysis was conducted. For the bare ZnO, the nanoparticles grown on the ITO substrate are separated without the template (Fig. 3a). On the contrary, the ZnO nanoparticles formed a continuous film in the presence of CNT with a low a root-mean-square (RMS) roughness value of 2.77 nm (Fig. 3b). Compared to ZnO@CNT-COOH, ZnO@CNT-Au reveals a similar morphology with increased roughness (Fig. 3c). Simultaneously, transmission electron microscopy (TEM) measurement was also carried out to clarify the growth of ZnO nanoparticles with CNT-COOH and CNT-Au inside (Fig. S2). In the corresponding HRTEM image of ZnO@CNT-Au, the (0002) lattice planes of ZnO (0.26 nm), the lattice fringes for the (111) planes of Au nanoparticle (0.23 nm) and graphite stacking of CNT (0.34 nm) confirm that the ZnO nanoparticles grown successfully inside the network of CNT-Au. It is found that ZnO nanoparticles tend to grow around the CNT. Besides, the addition of Au nanoparticles can also affect the wettability of the film. As depicted in Fig. S3, the contact angle of ZnO@CNT-COOH decreased a little because of the carboxylic CNT, but the contact angle of ZnO@CNT-Au increased, which attributed to the reduction of carboxylate groups during the dehydration-condensation reaction. In contrast, all the samples show no big difference in the crystallinity (Fig. S4).

The elemental composition of ZnO, ZnO@CNT-COOH and